

Bi-induced acceptor states in ZnO by molecular-beam epitaxy

F. X. Xiu, L. J. Mandalapu, Z. Yang, and J. L. Liu^{a)}

Quantum Structures Laboratory, Department of Electrical Engineering, University of California, Riverside, California 92521

G. F. Liu and J. A. Yarnoff

Department of Physics, University of California, Riverside, California 92521

(Received 28 February 2006; accepted 28 June 2006; published online 31 July 2006)

Bi-doped ZnO films were grown on Si (111) substrates by molecular-beam epitaxy. X-ray photoelectron spectroscopy and diffraction measurements reveal that Bi was incorporated into ZnO films without any phase separation. Room-temperature Hall effect measurements show a significant reduction of electron concentration and an increase of resistivity for Bi-doped ZnO films. In addition, a 3.222 eV photoluminescence emission was observed particularly in the Bi-doped ZnO films and was identified as a donor-acceptor pair transition by temperature-dependent and excitation power-dependent photoluminescence measurements. These results indicate the possibility of generating acceptor states by Bi doping. © 2006 American Institute of Physics.

[DOI: 10.1063/1.2243732]

Substantial research is currently being conducted worldwide on ZnO material for its potential applications in optoelectronics and spintronics. Towards these applications, *p*-type ZnO growth is an indispensable step to realize highly efficient devices. To date, group V elements N,^{1–4} P,^{5–11} As,^{12–15} and Sb,^{16–20} as well as group III-V codoping²¹ have been extensively attempted for producing *p*-type conductivity. However, Bi, the last element in group V, has rarely been tried in this regard. Traditionally, Bi-doped ZnO has long been used as the most important material for fabrication of varistors.²² It is known that Bi dopants can accumulate in the grain boundaries and form ZnO–Bi₂O₃ binary system to exhibit nonlinear *I*-*V* characteristics. A typical Bi percentage of 15%–30% in ZnO is needed to induce remarkable surface segregation and/or phase separation, thus producing varistor properties.²² However, for controlling conductivity in ZnO by Bi doping, the phase separation and/or surface segregation are undesirable. Duclere *et al.* tried Bi as *p*-type dopant by pulsed laser deposition technique.²³ The resulting Bi-doped ZnO films have a Bi percentage ranging from 1% to 4.3%. Unfortunately, all these films suffer from a phase segregation of β -tetragonal Bi₂O₃ and ZnO, leading to high resistivities and ambiguous carrier types. It was concluded that a lower doping concentration was needed to study Bi doping behavior. In this letter, we report the growth and characterizations of Bi-doped ZnO films on Si (111) substrates by an electron cyclotron resonance (ECR)-assisted molecular-beam epitaxy (MBE). The Bi percentage was well controlled below 0.4% to avoid any phase separation. X-ray photoelectron spectroscopy (XPS), x-ray diffraction (XRD), Hall effect, and low-temperature photoluminescence (PL) measurements were used to investigate the Bi doping behavior in ZnO.

Undoped and Bi-doped ZnO films were grown on Si (111) substrates at 550 °C. During growth, a high oxygen pressure of 1.3×10^{-3} Torr was used to depress the formation of Zn interstitials, and, hence, reduce the electron con-

centration in ZnO films. The other sources, namely, elemental zinc (6*N*) and bismuth (5*N*), were provided by conventional low-temperature effusion cells. The Si substrates are *n*-type wafers with high resistivity of 50–90 Ω cm. All substrates were cleaned by a Piranha-HF method and dried with nitrogen gas. The growth procedure is similar to our previous Sb-doped ZnO growth and the details are reported in Refs. 16 and 17. The total growth time was 2 h, giving a thickness of 660 nm.

XPS measurements were performed to detect the incorporation of Bi and investigate the local chemical bonding of Bi in ZnO. Figure 1 shows the XPS spectra of a heavily Bi-doped ZnO film (sample C in Table I). The inset presents a magnified spectrum with the scan range of 148–168 eV. A Bi characteristic peak was found at 158.1 eV (Bi 4*f*_{7/2}), indicating that Bi dopants were essentially incorporated into the ZnO film. An atomic percentage of 0.4% was estimated by integrating the peak intensities. Obviously Bi is not in a zero charge state (157 eV for Bi⁰).²⁴ With the observed value 158.1 eV closer to 158.8 eV (for Bi₂O₃),²⁵ it can be reasonably inferred that Bi has a positive charge state. This implies that Bi substitutes for Zn (Bi_{Zn}) and bonds with O. However, Bi₂O₃ phase separation is unlikely as proven in the following XRD experiments.

A Bruker advanced D8 x-ray diffractometer was used to examine the crystalline quality of all samples with a Cu *K* α

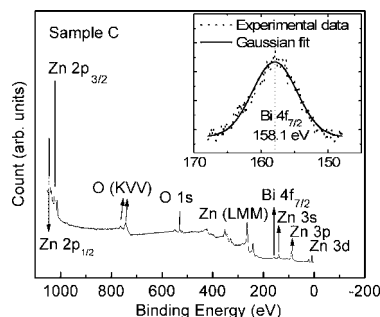


FIG. 1. Room-temperature XPS spectra of the heavily Bi-doped ZnO film (sample C). The inset is a magnified spectrum in the range of 148–168 eV.

^{a)} Author to whom correspondence should be addressed; electronic mail: jianlin@ee.ucr.edu

TABLE I. Electrical properties of undoped and Bi-doped ZnO films at room temperature.

Sample	Bi effusion cell		Carrier		
	temperature (°C)	Conduction type	concentration (cm ⁻³)	Mobility (cm ² /V s)	Resistivity (Ω cm)
A	N/A	<i>n</i>	2.7×10^{18}	7.4	0.3
B	340	<i>n</i>	4.4×10^{17}	5.4	2.6
C	400	<i>n</i>	9.1×10^{16}	15.9	4.3

radiation ($\lambda=1.5406 \text{ \AA}$). The resulting θ - 2θ spectra are shown in Figs. 2(a)–2(c), which correspond to the undoped (sample A), the lightly Bi-doped (sample B), and the heavily Bi-doped (sample C) ZnO films, respectively. It is found that all these films have a strong growth orientation along $\langle 002 \rangle$, i.e., the *c* axis, with diffraction angles of 34.60° , 34.45° , and 34.26° for samples A, B, and C, respectively. Based on these peak positions, the lattice constant *c* of 5.18, 5.21, and 5.23 \AA were calculated using Bragg's law. In comparison with the undoped ZnO film (sample A), the Bi-doped ZnO films show a slight increase of the lattice constant along the *c* axis, presumably due to the large atomic radius of Bi (1.63 \AA) compared with that of Zn (1.53 \AA) and O (0.73 \AA). In addition, the full width at half maximum (FWHM) value increases with the higher Bi effusion cell temperature (0.22° and 0.25° for samples B and C, respectively), indicating the incorporation of Bi dopants. Moreover, with the spectra ranging from 25° to 45° , no β -tetragonal ($2\theta=27.947^\circ$) and α -monoclinic ($2\theta=28.001^\circ$) phases of Bi_2O_3 were observed for all Bi-doped ZnO films.

Hall effect measurement was carried out to characterize the electrical properties of all ZnO films with an HMS-3000 Hall effect measurement system. All samples were prepared in a van der Pauw configuration. Table I summarizes the growth conditions and electrical data of the undoped and Bi-doped ZnO films at room temperature. The undoped ZnO film has an *n*-type conductivity with an electron concentration of $2.7 \times 10^{18} \text{ cm}^{-3}$, a mobility of $7.4 \text{ cm}^2/\text{V s}$, and a resistivity of 0.3 \Omega cm . High electron concentration in this film may be attributed to the incorporation of residual H impurities during growth, which could serve as shallow donors to provide electrons.²⁶ The Bi-doped ZnO films, however, show a significant reduction of electron concentrations with values of 4.4×10^{17} and $9.1 \times 10^{16} \text{ cm}^{-3}$ for the lightly and heavily Bi-doped ZnO films, respectively. Accordingly,

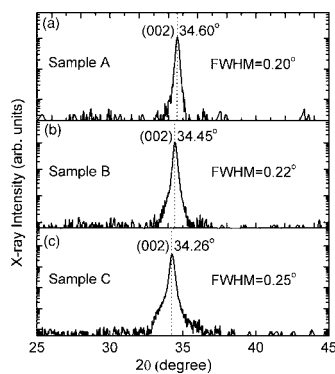


FIG. 2. X-ray θ - 2θ scans of the undoped (sample A) and Bi-doped (samples B and C) ZnO films grown on Si (111) substrates. ZnO (002) peak position shifts to smaller diffraction angles with Bi doping, indicating the incorporation of Bi dopants.

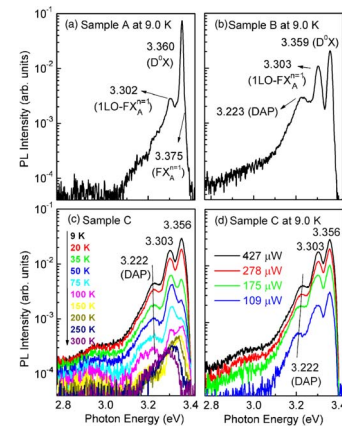


FIG. 3. (Color online) Low-temperature PL spectra of (a) the undoped ZnO film at 9.0 K (sample A), (b) the lightly Bi-doped ZnO film at 9.0 K (sample B), (c) the heavily Bi-doped ZnO film at temperatures ranging from 9 to 300 K (sample C), and (d) the heavily Bi-doped ZnO film with different excitation power at 9.0 K (sample C). At 9.0 K, the FWHM values of D^0X emissions are 9, 20, and 36 meV for samples A, B, and C respectively.

the resistivity and mobility values change with the incorporation of Bi dopants, as shown in Table I. In fact, the reduction of electron concentration is not unusual as it was widely observed in P- (Refs. 6, 8, and 11) and Sb-doped²⁰ ZnO films; and till now, it is understood that this phenomenon mainly arises from the compensation effect due to the generation of acceptor states originated from P and Sb doping.^{8,19} However, since the number of the acceptor states cannot exceed the number of existing electrons in conduction band, the macroscopic and homogeneous *p*-type conductivity cannot be obtained.

To confirm the formation of acceptor states by Bi doping, low-temperature PL measurements were conducted with a 325 nm He–Cd laser operated at 0.43 mW. The laser beam was impinged on the sample surface with an angle of approximately 60° . The excited PL emission was measured with an Oriel monochromator, aligned normal to the sample surface. Figures 3(a)–3(c) show the low-temperature PL spectra for samples A–C, respectively. Based on peak assignments in Ref. 27 and our previous study in Ref. 17, PL emissions at 3.360, 3.375, and 3.302 eV in Fig. 3(a) can be ascribed to donor-bound exciton (D^0X), ground state of A free exciton ($FX_A^{n=1}$), and LO-phonon replica of the ground state A exciton ($1LO-FX_A^{n=1}$), respectively. The appearance of different states of free exciton reflects the good optical property of the undoped ZnO film. For the Bi-doped ZnO films, however, the D^0X emission shows a slight redshift with peak positions at 3.359 eV for the lightly doped ZnO and 3.356 eV for the heavily doped ZnO, as seen in Figs. 3(b) and 3(c), respectively. Similar to the scenario of P-doped ZnO,¹¹ this shift might indicate the compensation nature of Bi doping. It is also noticed that, different from the undoped ZnO, the Bi-doped ZnO films show another emission at about 3.222 eV [Figs. 3(b) and 3(c)]. As a matter of fact, emissions with similar photon energies were reported in N-doped (3.216 eV),²⁸ P-doped (3.241 eV),⁵ As-doped (3.204 eV),¹² and Sb-doped (3.222 eV) (Refs. 16 and 17) ZnO films and were identified as donor-acceptor pair (DAP) transitions.

Temperature-dependent PL measurements were used to investigate the nature of this emission at the temperature ranging from 9 to 300 K, as shown in Fig. 3(c). It is found

that with an increase of temperatures from 9 to 100 K, the 3.222 eV emission line shows a progressive blueshift as a result of thermal ionization of donors at higher temperatures; this characteristic has been routinely reported as the typical feature of the DAP transition for ZnO (Refs. 29 and 30) and GaN (Ref. 31) material systems.

The DAP nature of this emission can also be proven by excitation power-dependent PL measurements. The experiments were carried out at 9.0 K with different laser excitation power, as shown in Fig. 3(d). With an increase of the excitation power, the 3.222 eV emission shows an evident blueshift. This phenomenon is again quite consistent with the characteristics of a DAP transition, whose energy is represented by the following equation:⁵

$$E_{\text{DAP}} = E_G - (E_D + E_A) + \frac{e^2}{4\pi\epsilon r_{\text{DAP}}},$$

where E_{DAP} , E_G , E_D , E_A , e , ϵ , and r_{DAP} are DAP transition energy, band gap energy, donor ionization energy, acceptor ionization energy, elementary electrical charge, dielectric constant, and donor-acceptor pair distance, respectively. As the excitation intensity (power/area) increases, the number of photoexcited donor-acceptor pairs increases, giving rise to a shorter donor-acceptor pair distance (r_{DAP}). Therefore, a DAP transition shifts to a higher energy.

Based on the DAP peak position in our Bi-doped ZnO films, the Bi-induced acceptor binding energy can be estimated to be 185–245 meV.^{3,16} The formation of shallow acceptor levels in the Bi-doped ZnO films can be understood in the following way. XPS results show that Bi in ZnO films has positive charge state. This indicates that Bi_{Zn}, rather than Bi_O, is formed in the films. Bi_{Zn} itself, however, is a donor, which would provide electrons. A dramatic reduction in electron concentration in our Bi-doped samples suggests that isolated Bi_{Zn} should not exist in a large amount. Due to oxygen-rich growth conditions used for the Bi-doped ZnO films, Bi_{Zn} may connect with other point defects such as Zn vacancies (V_{Zn}) or O interstitials (O_i) to form Bi_{Zn}- V_{Zn} - O_i and/or Bi_{Zn}-2 V_{Zn} defect complexes. From the first principles,^{32,33} these defect complexes are inferred to produce shallow acceptor states.

In summary, we report the growth and characterizations of Bi-doped ZnO films on Si (111) by ECR-assisted MBE. A low-temperature Bi effusion cell was used to provide Bi dopants. The XPS and XRD measurements indicate that Bi dopants were incorporated into ZnO films, and the ZnO lattice constant c increases with higher Bi doping. The room-temperature Hall effect measurements demonstrate that the undoped ZnO sample has a high electron concentration of $2.7 \times 10^{18} \text{ cm}^{-3}$ and a low resistivity of 0.3 $\Omega \text{ cm}$. The Bi-doped ZnO films, however, show a dramatic reduction of electron concentration with the increase of Bi incorporation. The low-temperature PL measurements reveal a strong D^0X emission at 3.360 eV for the undoped ZnO and 3.356–3.359 eV for the Bi-doped ZnO films. A 3.222 eV emission was found in the Bi-doped ZnO films and was identified as a DAP transition by the temperature-dependent and excitation power-dependent PL measurements. These results indicate that Bi doping can introduce shallow acceptor states in ZnO films, and hence dramatically compensate the background electrons. Therefore, Bi doping could be a practical approach for realizing p -type ZnO.

This work was supported by DARPA/DMEA through the Center for NanoScience and Innovation for Defense (CNID) under the Award No. H94003-04-2-0404 and by DMEA through the Center of Nanomaterials and Nanodevices (CNN) under the Award No. H94003-05-2-0505.

- ¹A. Tsukazaki, A. Ohtomo, T. Onuma, M. Ohtani, T. Makino, M. Sumiya, K. Ohtani, S. F. Chichibu, S. Fuke, Y. Segawa, H. Ohno, H. Koinuma, and M. Kawasaki, *Nat. Mater.* **4**, 42 (2005).
- ²J. M. Bian, X. M. Li, C. Y. Zhang, W. D. Yu, and X. D. Gao, *Appl. Phys. Lett.* **85**, 4070 (2004).
- ³D. C. Look, D. C. Reynolds, C. W. Litton, R. L. Jones, D. B. Eason, and G. Cantwell, *Appl. Phys. Lett.* **81**, 1830 (2002).
- ⁴J. G. Lu, Z. Z. Ye, F. Zhuge, Y. J. Zeng, B. H. Zhao, and L. P. Zhu, *Appl. Phys. Lett.* **85**, 3134 (2004).
- ⁵D. K. Hwang, H. S. Kim, J. H. Lim, J. Y. Oh, J. H. Yang, S. J. Park, K. K. Kim, D. C. Look, and Y. S. Park, *Appl. Phys. Lett.* **86**, 151917 (2005).
- ⁶V. Vaithianathan, B. T. Lee, and S. S. Kim, *Phys. Status Solidi A* **201**, 2837 (2004).
- ⁷K. K. Kim, H. S. Kim, D. K. Hwang, J. H. Lim, and S. J. Park, *Appl. Phys. Lett.* **83**, 63 (2003).
- ⁸H. Tambo, H. Shibata, P. Fons, A. Yamada, K. Matsubara, K. Iwata, K. Tamura, H. Takasu, and S. Niki, *J. Cryst. Growth* **278**, 268 (2005).
- ⁹Y. J. Li, Y. W. Heo, Y. Kwon, K. Ip, S. J. Pearton, and D. P. Norton, *Appl. Phys. Lett.* **87**, 072101 (2005).
- ¹⁰F. X. Xiu, Z. Yang, L. J. Mandalapu, J. L. Liu, and W. P. Beyermann, *Appl. Phys. Lett.* **88**, 052106 (2006).
- ¹¹F. X. Xiu, Z. Yang, L. J. Mandalapu, and J. L. Liu, *Appl. Phys. Lett.* **88**, 152116 (2006).
- ¹²Y. R. Ryu, T. S. Lee, and H. W. White, *Appl. Phys. Lett.* **83**, 87 (2003).
- ¹³D. C. Look, G. M. Renlund, R. H. Burgener II, and J. R. Sizelove, *Appl. Phys. Lett.* **85**, 5269 (2004).
- ¹⁴T. S. Jeong, M. S. Han, C. J. Youn, and Y. S. Park, *J. Appl. Phys.* **96**, 175 (2004).
- ¹⁵G. Braunstein, A. Muraviev, H. Saxena, N. Dhere, V. Richter, and R. Kalish, *Appl. Phys. Lett.* **87**, 192103 (2005).
- ¹⁶F. X. Xiu, Z. Yang, L. J. Mandalapu, D. T. Zhao, J. L. Liu, and W. P. Beyermann, *Appl. Phys. Lett.* **87**, 152101 (2005).
- ¹⁷F. X. Xiu, Z. Yang, L. J. Mandalapu, D. T. Zhao, and J. L. Liu, *Appl. Phys. Lett.* **87**, 252102 (2005).
- ¹⁸T. Aoki, Y. Shimizu, A. Miyake, A. Nakamura, Y. Nakanishi, and Y. Hatanaka, *Phys. Status Solidi B* **229**, 911 (2002).
- ¹⁹K. Ohara, T. Seino, A. Nakamura, T. Aoki, H. Kominami, Y. Nakanishi, and Y. Hatanaka, *Appl. Surf. Sci.* **244**, 369 (2005).
- ²⁰T. M. Borseth, J. S. Christensen, K. Maknys, A. Hallen, B. G. Svensson, and A. Y. Kuznetsov, *Superlattices Microstruct.* **38**, 464 (2005).
- ²¹J. G. Lu, Z. Z. Ye, F. Zhuge, Y. J. Zeng, B. H. Zhao, and L. P. Zhu, *Appl. Phys. Lett.* **85**, 3134 (2004).
- ²²A. Gulino and I. Fragala, *Chem. Mater.* **14**, 116 (2002).
- ²³J. R. Duclere, R. O. Haire, A. Meaney, K. Johnston, I. Reid, G. Tobin, J. P. Mosnier, M. G. Viry, E. Mcglynn, and M. O. Henry, *J. Mater. Sci.* **16**, 421 (2005).
- ²⁴J. C. Fuggle and N. Martensson, *J. Electron Spectrosc. Relat. Phenom.* **21**, 275 (1980).
- ²⁵Fundamental XPS data from pure elements, pure oxides, and chemical compounds, copyrights 1999 XPS International Inc., <http://www.xpsdata.com/fundxps.pdf>
- ²⁶C. G. Van de Walle, *Phys. Rev. Lett.* **85**, 1012 (2000).
- ²⁷Ü. Özgür, Ya. I. Alivov, C. Liu, A. Teke, M. A. Reshchikov, S. Doğan, V. Avrutin, S.-J. Cho, and H. Morkoç, *J. Appl. Phys.* **98**, 041301 (2005).
- ²⁸L. J. Wang and N. C. Giles, *Appl. Phys. Lett.* **84**, 3049 (2004).
- ²⁹K. Tamura, T. Makino, A. Tsukazaki, M. Sumiya, S. Fuke, T. Furumochi, M. Lippmaa, C. H. Chia, Y. Segawa, H. Koinuma, and M. Kawasaki, *Solid State Commun.* **127**, 265 (2003).
- ³⁰K. Thonke, T. Gruber, N. Teofilov, R. Schonfelder, A. Waag, and R. Sauer, *Physica B* **308**, 945 (2001).
- ³¹P. W. Yu, C. S. Park, and S. T. Kim, *J. Appl. Phys.* **89**, 1692 (2001).
- ³²J. M. Carlsson, H. S. Domingos, P. D. Bristowe, and B. Hellsing, *Phys. Rev. Lett.* **91**, 165506 (2003).
- ³³S. Limpijumnong, S. B. Zhang, S. H. Wei, and C. H. Park, *Phys. Rev. Lett.* **92**, 155504 (2004).